

Uncertainty Evaluation in a Two-Terminal Cryogenic Current Comparator

M. E. Bierzychudek and R. E. Elmquist, *Senior Member, IEEE*

Abstract— We present an uncertainty evaluation of a new cryogenic current comparator (CCC) bridge designed to compare two-terminal 1 M Ω and 10 M Ω standard resistors with the quantized Hall resistance (QHR) and scale from these decade values to other decade values between 10 k Ω and 1 G Ω . Use of the bridge over a wide range of resistance values results in a spectrum of dominant contributions to the uncertainty budget, and this analysis helps to determine the optimum parameters of the measurements. Our theoretical analysis is compared with experimental data.

Index Terms—Uncertainty, Current comparators, Resistance measurement, SQUIDS, Noise

I. INTRODUCTION

THE CCC bridge is used widely in metrology to obtain high accuracy resistance ratios, typically in the range of 1 Ω to 10 k Ω . The CCC can also be used to measure high value resistors [1] and small currents [2]; however the traditional bridge design in some ways is less than ideal for high resistance. Uncertainty due to electrical leakage currents in these bridges [3] can be largely eliminated by using a CCC that compares two-terminal high-value resistance standards. In particular, the effect of leakage current is greatly reduced by using a single voltage source, instead of two isolated current sources. This also simplifies the electronics design and can reduce instability in the critical bridge feedback circuit, which is based on a superconducting quantum interference device (SQUID).

Two-terminal CCC bridges have been described in [4] that compare the QHR standard directly with 1 M Ω and 100 M Ω resistors. One of these used resistive wire for the ratio winding with the largest number of turns, giving a reduced quality factor (Q) in that winding. Since high- Q

windings provide no benefit at dc and can produce resonances [5] that destabilize the SQUID, the resistive-winding technique is adapted here for use in a CCC with multiple ratio windings. This paper presents a complete study of the uncertainty in a two-terminal CCC with multiple ratios, which provide new capabilities in resistance scaling for high-value resistors [6-7].

II. CCC BRIDGE OVERVIEW

Figure 1 shows a schematic diagram of the two-terminal CCC described in this work. The source voltage is applied directly to the two resistors under test, in parallel. Each resistor is in series with a winding in one arm of the bridge, and these two windings have opposite directions and are tied together at a superconducting point connected to the low of the source, which is grounded. A dc SQUID magnetic flux detector senses the net flux produced in the CCC when the voltage is applied, and drives a feedback winding of one turn to maintain a constant flux balance in the bridge. This feedback current is measured, and then measured again after the source voltage is ramped to a similar dc output level with the opposite sign. The known ratio of the CCC windings allows the resistance ratio of the two bridge arms to be calculated from the change in the feedback current between the two dc voltage states and the applied voltage difference.

This bridge uses six major windings. The four-turn winding is superconducting and is used with the QHR standard. The 3100-turn, 310-turn and 31-turn windings used with room-temperature standard resistors are made of phosphor-bronze wire and have nominal resistance values

Manuscript received June 3, 2008.

M. E. Bierzychudek is with the Instituto Nacional de Tecnología Industrial, San Martín, B1650KNA, República Argentina (54-11-4724-6200, marcosb@inti.gov.ar).

R. E. Elmquist is with the National Institute of Standards and Technology, Gaithersburg, MD, USA (301-975-6591, elmquist@nist.gov). Official contribution of the National Institute of Standards and Technology, not subject to copyright in the United States.

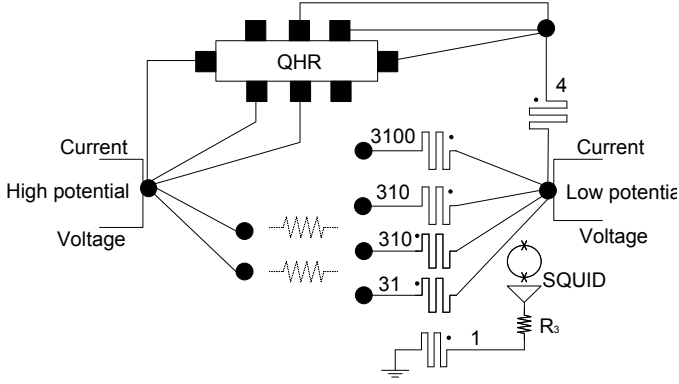


Fig. 1. Diagram of the two-terminal CCC showing connections of the QHR and standard resistors. Note that only two of the five ratio arms are used simultaneously and the CCC windings in those arms must have opposite directions, and only the 3100-turn or upper 310-turn winding can be used in the primary bridge arm.

at 4.2 K of 2500 Ω , 250 Ω and 25 Ω , respectively. The internal resistances of the windings greatly decrease the effect of self-resonance in the CCC and this makes it possible to use windings of high inductance that improve the sensitivity without introducing excess noise. Since this bridge measures two-terminal resistors, the winding resistances must be measured separately to obtain a correction to the measured value of each room-temperature resistor.

The bridge can be connected to measure a 1 M Ω or 10 M Ω room-temperature resistor against the QHR standard on the $i=2$ plateau (12906.4035 Ω) with a winding ratio of 310-to-4 or 3100-to-4. We use the triple-series connection technique to reduce errors due to lead resistance in measurements with the QHR, as described in [4], and the triple series connection is made at the two bridge superconducting junctions in the cryogenic environment of the CCC.

In a condition of balance, the bridge equations are:

$$I_1 N_1 = I_2 N_2 + I_F N_F + \Delta, \quad (1)$$

$$I_1 = \frac{V}{R_1 + r_{w1}}, \quad I_2 = \frac{V}{R_2 + r_{w2}}. \quad (2)$$

Here, I_j is the current in the resistor j , r_{wj} is the resistance in the connections of the j bridge arm, N_j is the number of turns in the winding j , V is the source voltage, I_F is the feedback current and Δ includes all systematic contributions. We can solve the bridge equations above to find the resistance R_1 ,

$$R_1 = \frac{VN_1}{VN_2/(R_2 + r_{w2}) - I_F N_F + \Delta} - r_{w1}. \quad (3)$$

III. UNCERTAINTY COMPONENTS

A. Type A evaluation of standard uncertainty.

First, we describe components which produce random errors in the result and can be reduced by averaging. This

set of noise components contributes to the standard deviation of measurements closely spaced in time, and is calculated as the standard deviation within a set of data.

• **Johnson-Nyquist noise.** The noise current produced by a resistor R_j , with a temperature T and a bandwidth BW is

$$I_n = \sqrt{\frac{4 k_B T BW}{R_j}}, \quad (4)$$

where k_B is the Boltzmann constant. The standard deviation of the Johnson noise is multiplied by the number of turns N_j in the winding and divided by a current sensitivity factor f_{CCC} to obtain the flux in the SQUID loop produced by the Johnson current,

$$u_{in} = \sqrt{\frac{4 k_B T BW}{R_j} \left(\frac{N_j}{f_{CCC}} \right)}. \quad (5)$$

The Johnson noise does not produce correlation among the samples so when we average samples we can decrease the effect of this noise. In the system described here, the factor f_{CCC} is approximately 3.81×10^{-6} A-turn/ Φ_0 , where Φ_0 is the flux quantum.

• **Electromagnetic interference (EMI) and vibration noise.** These types of interference are very difficult to estimate and a well-tested design is necessary to minimize these effects. The liquid-helium cooled region of the CCC is surrounded by several levels of superconductive shielding. All the wires connecting the CCC with the electronics or the resistors are shielded and twisted. The interconnecting leads inside the CCC cryostat are isolated by fine tubing as necessary but are twisted together and fixed to the CCC probe.

• **CCC electronics: voltage source and feedback current.** The voltage source and the feedback current source were designed using low pass filters and low noise components. We made all the ground connections with very low impedance paths to reduce noise between grounds. Inside the cabinet the interconnecting wires and circuit boards were shielded from other nearby components.

• **SQUID and electronics.** The dc SQUID system produces 1/f and white noise components specified by the manufacturer in units of $\Phi_0/\text{Hz}^{1/2}$. The current reversal technique helps to eliminate the slowly changing offset in the SQUID, but the 1/f noise is not totally eliminated with this technique. The white noise of the SQUID magnetic flux detector is specified to be below 5 $\mu\Phi_0/\text{Hz}^{1/2}$, with a 1/f noise corner near 0.4 Hz and an output gain of 0.77 V/ Φ_0 .

We measured the SQUID output voltage to characterize the SQUID and semi-isolated CCC system noise. In these measurements the cryostat was only connected to the SQUID electronics, and the output of the SQUID electronics was measured with a digital multimeter (DMM). A histogram of voltage readings from the SQUID are shown in Fig. 2. This data is typical for measurement integration periods of 5 s, with delay times between measurements of 4 s to 30 s, and shows that the noise in the SQUID signal can be modeled with a Gaussian probability density function with a mean value of 0 V and a standard deviation of 30 μV . The excess contribution of EMI and

vibration-induced noise is probably evident here, and is also seen as noise peaks at frequencies between 1 Hz and 500 Hz in power spectral density measurements.

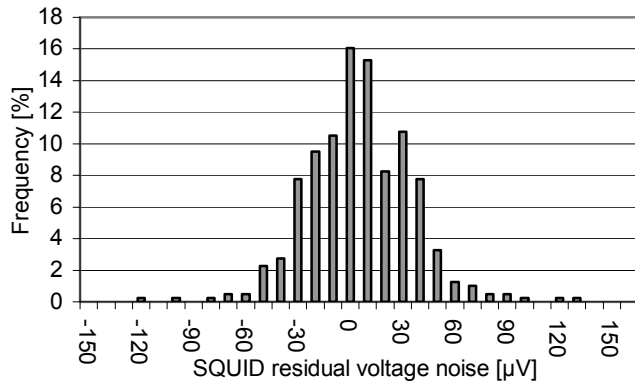


Fig. 2. Histogram showing the distribution of noise voltage measurements made at the output of the dc SQUID. We eliminate the slowly changing voltage offset by taking a difference of three samples: the first is the average value of N readings, the second is the average value of $2*N$ readings and the last sample is the average value of N readings. The plotted data consists of 399 samples with 30 s of delay between samples with $N = 5$ seconds integration time. We obtained a mean of $0.59 \mu\text{V}$ and a standard deviation of $30 \mu\text{V}$.

B. Type B evaluation of standard uncertainty.

This type of component can produce a systematic offset in the result. The physical process that causes an offset can sometimes be modeled and a calculated correction can be applied to reduce the uncertainty.

- **Winding and lead resistance.** The uncertainty produced by the correction of the winding and lead resistance has three components: the measurement device, the current coefficient of resistance and the dependence on helium level. For the windings and connecting leads that are made of phosphor-bronze wire the change of resistance is in the range of one or two milliohms when the helium level changes from 100% to 10%. This effect is due mainly to the leads that connect the windings with the connectors in the top of the cryostat. This error can be eliminated if the resistance is measured each day.

We have compared several different methods of measuring the resistance of the connecting leads and windings, and found that high-resolution DMMs provide good sensitivity and accuracy using the four-terminal resistance function. A settling delay of up to 10 s is necessary before each reading for the 3100-turn winding and lead resistance. The estimated total relative uncertainty (1σ) of the resistance corrections is $10 \mu\Omega/\Omega$ for the 31 turn arm of the bridge, $10 \mu\Omega/\Omega$ for the 310 turn arm and $20 \mu\Omega/\Omega$ for the 3100-turn arm.

The uncertainty of the 31-turn lead and winding resistance is critical when it is connected to a $10 \text{ k}\Omega$ resistance standard. Here, potentiometer measurements may be more accurate than the resistance function of the DMM. In this method the standard resistor's four-wire terminations provide taps for measuring the voltage drops produced in the connecting wiring, using the voltage source as in a

normal CCC measurement. The DMM measures the voltage drop from the appropriate potential point of the bridge to the unused high and low potential taps of the resistor for both current directions, and these are used to calculate the resistance correction of the bridge arm.

To estimate the current coefficient we measure each winding with different currents. We have found that the effect of the current is only important in the 3100-turn winding, and its relative current coefficient is $4 \times 10^{-7} \Omega/\mu\text{A}$. Typically, we measure the 3100 winding with a current of $50 \mu\text{A}$, and in use it carries currents lower than $10 \mu\text{A}$, so this uncertainty is $20 \mu\Omega/\Omega$. This winding is typically used with resistor values greater than $1 \text{ M}\Omega$, so the systematic uncertainty produced by the current coefficient is approximately $0.005 \mu\Omega/\Omega$ or less.

- **Measurement of the feedback current.** To measure the feedback current we use a $200 \text{ k}\Omega$ sense resistor and two buffers, one at each resistor terminal, and a multimeter that measures the difference voltage between the outputs of the buffers. These buffers produce errors due to their bias currents, as well as high frequency voltage noise and $1/f$ noise due to the temperature dependence of the voltage offset. These last two produce a very small error but the buffer bias current limits the uncertainty in some high resistance measurements where both the measurement currents and feedback current are small. One of these buffers is between the sense resistor and the feedback current source and the other is between the resistor and the 1-turn feedback winding. The first does not produce an error because it is before the sense resistor, however the bias current of the second buffer changes the sensed current, and it produces an error that we estimate like a flux error. The sense resistor is a stable, card-type wire-wound resistor with a temperature coefficient of less than $1 (\mu\Omega/\Omega)/^\circ\text{C}$ and its value has a negligible uncertainty contribution. Thus, the uncertainty of the feedback current measurement is calculated as the uncertainty produced by the DMM and the buffer bias current.

- **Voltage source and thermal EMF.** This type of bridge does not use a feedback loop with a third winding to balance the voltage across each resistor; instead the voltage balance is created at the two superconducting junctions linking the arms of the bridge. The stability of the bridge voltage is best when using the voltage compensation technique, where the source output buffer senses the feedback voltage directly from the two superconducting junction points of the bridge.

Like the primary source in any current comparator bridge, the instability of the source produces an uncertainty that is proportional to the resistance ratio imbalance. In addition, the voltage across each resistor can be affected by the thermal electromotive forces (EMF) in the arms of the bridge. These effects are reduced by the bridge voltage reversals if the voltage source and thermal EMF are constant or drift linearly. We have found a stability of 5 nV in the EMF of the bridge connections which produces less than $0.001 \mu\Omega/\Omega$ uncertainty at 10 V bridge voltage. The

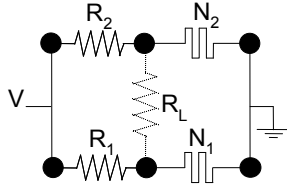


Fig. 3a.

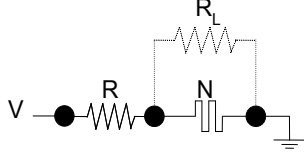


Fig. 3b.

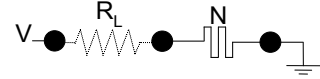


Fig. 3c.

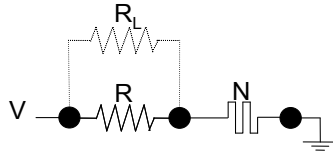


Fig. 3d.

voltage source stability is better than 25 μV after an initial warm-up of 45 minutes, which produces a similar level of uncertainty.

• **Leakage current.** In this CCC the leakage current can affect only in four different situations. The first two are different to a traditional superconducting CCC and more similar to a Direct Current Comparator since some windings are resistive.

a) The first situation is for a leakage current I_L between different windings (see Fig. 3a), which can be estimated as

$$I_L \cong \frac{1}{R_L} \left(\frac{VR_{N1}}{R_1 + R_{N1}} - \frac{VR_{N2}}{R_2 + R_{N2}} \right), \quad (6)$$

where V is the source voltage, R_{Nj} is the resistance in the winding j plus the lead resistance and R_j is the resistance of the standard in the j bridge arm. The systematic error in the ratio is then

$$e_r = \frac{(I_L N_1 + I_L N_2)}{(VN_1/R_1)} \cong \left(\frac{R_{N1}}{R_L} - \frac{R_{N2}}{R_L} \frac{R_1}{R_2} \right) \left(1 + \frac{N_2}{N_1} \right). \quad (7)$$

A slightly different case is when one of the windings is not used,

$$I_L \cong \frac{1}{R_L} \left(\frac{VR_{N1}}{R_1 + R_{N1}} \right), \quad (8)$$

$$e_r \cong \frac{R_{N1}}{R_L} \left(1 + \frac{N_2}{N_1} \right). \quad (9)$$

In both case, the error is small because the point of leakage is close to ground potential. This leakage current is limited by grounded shields or polytrifluoroethylene (PTFE) insulation surrounding the bridge conductors in all regions except in the contacts between the windings inside the CCC. In this region the wires are at 4.2 K and we have

measured this isolation resistance using an electrometer and found a minimum value of 10 T Ω . With a leakage resistance of 10 T Ω the relative error is less than 0.001 $\mu\Omega/\Omega$.

b) Leakage through isolation resistance in parallel to a winding (Fig. 3b) produces a current divider between the winding resistance (R_{Nj}) and the leakage resistance.

$$I_L = I_j \frac{R_{Nj}}{R_L + R_{Nj}}, \quad (10)$$

$$e_r = \frac{R_{Nj}}{R_L + R_{Nj}}. \quad (11)$$

The most likely location of this type of leakage current is between the turns of the windings. We cannot measure this isolation resistance but we know that it should be on the order of the resistances isolation between windings. The uncertainty increases with R_{Nj} and is greatest for $R_{Nj} \approx 2500 \Omega$, and this error is 0.00025 $\mu\Omega/\Omega$ with an isolation resistance of 10 T Ω . We use thick Formvar insulated wires to wind the CCC, and the specification of resistivity for this material is $1 \cdot 10^{17} \Omega\text{cm}$ at ambient temperature. It is important to note that this error is independent of the resistor under test.

c) When a winding is not used, a leakage current could flow from the positive terminal of the source to the positive terminal of the winding (Fig. 3c) and produce an error as it flows in the winding. Inside the CCC probe, all of the Formvar-insulated wires used to connect the resistors are in separate PTFE tubes giving very low leakage current. The cable terminations of all of the decade-value windings are shielded PTFE-insulated coaxial connectors on the top flange of the CCC probe, eliminating any source of such leakage. The three positive terminations that allow the QHR standard to be connected to the CCC are made at a shielded, multi-pin connector which also carries the source voltage. Because of this construction difference, the leakage problem is more important in the QHR coil (4-turn) and also the feedback coil (1-turn). The relative error produced by this current leakage can be estimated as the flux produced in the 4-turn plus 1-turn windings by a current that flows in the isolation resistance with due to the source voltage,

$$e_r = \frac{5V}{R_L} \frac{N_1 V}{R_1} = \frac{R_1}{R_L} \frac{5}{N_1}. \quad (12)$$

The insulation of the multi-pin connector is improved by selected grouping the pins and is measured to be greater than 10 T Ω . Thus, this error is less than 0.2 $\mu\Omega/\Omega$ for ratios involving a 1 G Ω primary resistor.

d) Leakage in parallel to the resistors under test (Fig. 3d) can be caused by surface conduction of the resistor element, with an uncertainty that can be made negligible by the resistor's construction, or conduction through insulators used in mounting the resistor. The second of these can be intercepted by grounded or guarded conductors. Leakage from the high resistor terminal to a grounded conductor is in parallel to the source voltage and thus does not produce a

significant error.

Guarding is necessary with this design of CCC only for high-resistance Hamon network devices [8, 9] with multiple internal connections, where leakage through an isolation resistance causes current to flow through a major part of the resistor under test. Internal or external guard networks are often used to decrease the effect of the leakage current. The CCC voltage source provides a guard voltage output to drive a guard network and reduce the leakage current uncertainty, which can be of order $5 \mu\Omega/\Omega$ for an unguarded Hamon device of $1 \text{ G}\Omega$ series resistance. The residual error with a guard network matched to 1% would be of order $0.05 \mu\Omega/\Omega$.

- **CCC current-linkage error.** With effective shielding, reversing the current passing through two windings of equal number in series-opposition should produce no change in the voltage output of the SQUID, when it is not connected to the feedback circuit. To test this, the CCC solenoid was constructed with an additional five superconducting windings: two of 1-turn, two of 2-turn and one of 4-turn. A build-up procedure was used where currents from the reversing source were applied and the SQUID output voltage was measured. We used a resistor in series with the voltage source to limit the current to 5 mA or 10 mA. The estimated relative uncertainty was calculated as the flux mismatch divided by the total theoretical flux, and was approximately $0.005 \mu\Omega/\Omega$ or less.

- **SQUID feedback null.** Upon the reversal of the voltage source, the external feedback must maintain constant output voltage in the SQUID electronics. We can make the same measurement as for SQUID 1/f noise but with the feedback on, which tests the operation of the feedback integrator. It is important to note that with feedback on, the SQUID output voltage is more constant than without feedback. This means that the SQUID 1/f noise is cancelled by the feedback and it is transferred to the voltage in the current sense resistor. No difference upon current reversal greater than the measurement uncertainty of $1.5 \mu\text{V}$ was detected in the SQUID output. This is equivalent to an uncertainty of about $0.08 \mu\Omega/\Omega$ in a 1-to-1 ratio at $100 \text{ M}\Omega$ and 10 V , using 310-turn windings.

- **Resistor under test.** Resistors of value higher than $1 \text{ M}\Omega$ in particular can exhibit a time constant of resistance, due to dielectric absorption after the measurement voltage is applied. We have seen excellent results with no measurable time constant in standard resistors up to $1 \text{ G}\Omega$ constructed using metal film resistors [10, 11]. In this analysis we do not consider the effect of the temperature coefficient of resistance in the resistors under test, and this can increase the total uncertainty.

- **QHR, triple-series connection.** The relative change in the quantized Hall resistance using a triple-series connection for DC measurements, compared to a four-terminal resistance measurement, can be calculated from a mathematical model of the QHR [12, 13]. We estimate this difference to be less than $0.001 \mu\Omega/\Omega$ for this CCC when using typical QHR lead resistance and longitudinal

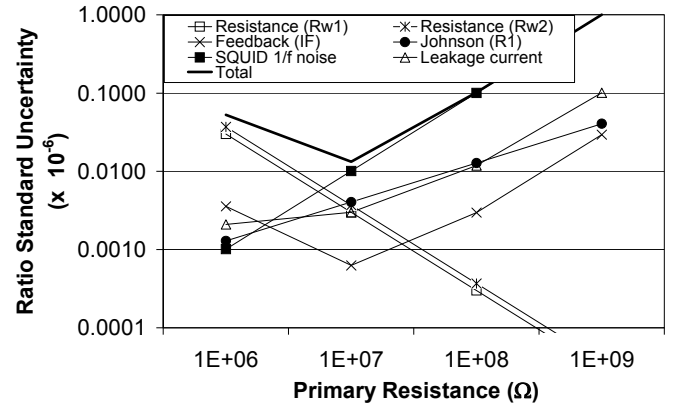


Fig. 4. The seven most significant uncertainty contributions derived in the simulation, for 100-to-1 resistance ratios using the 3100-turn and 31-turn CCC windings. The contributions are derived for a 10 V source voltage and for sequences of 24 readings each having 4 s DMM integration time. The total uncertainty includes all factors described in the text.

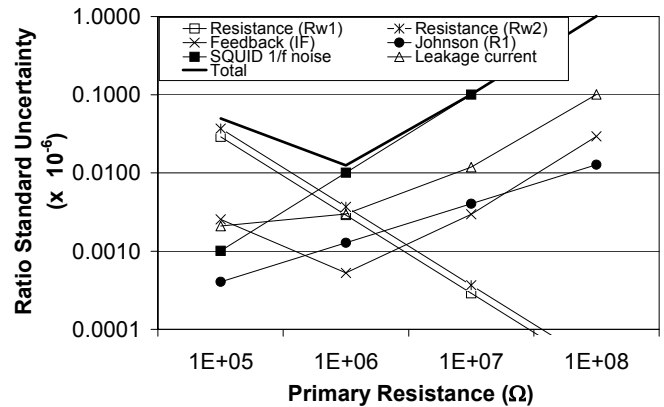


Fig. 5. Significant uncertainty contributions derived in the simulation, for 10-to-1 ratios using the 310-turn and 31-turn CCC windings. The contributions are derived for a 10 V source voltage and for sequences of 24 readings each having 4 s DMM integration time. The total uncertainty includes all factors described in the text. Note the total uncertainty is a minimum at a primary resistance of $1 \text{ M}\Omega$, while the minimum is at $10 \text{ M}\Omega$ in Fig. 4.

resistance values.

Calculations of the combined standard uncertainty for the many combinations of windings, resistance values, and measurement parameters were condensed into spreadsheet form, which simplifies the calculation of uncertainty terms. Graphs of the largest contributions in the simulated uncertainty calculations are shown for two important cases in Fig. 4 and Fig. 5. Comparing these figures shows that for resistance comparisons at values of $10 \text{ M}\Omega$ and above, ratios which use the 3100-turn winding should yield the lowest uncertainty. For scaling involving only standard resistors of $1 \text{ M}\Omega$ and below, better results may be produced using the lower 10-to-1 ratio, with the 310-turn winding in the primary arm, because of smaller winding resistance uncertainty.

The QHR to $1 \text{ M}\Omega$ and $10 \text{ M}\Omega$ ratios eliminate the secondary arm resistance correction, but the voltage source output must be limited to about 1 V to maintain ideal contact resistance and longitudinal resistance in the QHR

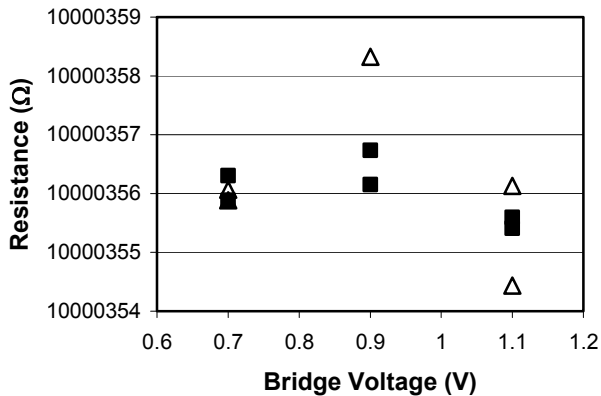


Fig. 6. Resistance values for a 10 M Ω resistance standard measured using direct scaling from the QHR standard (solid squares) and by scaling from the QHR using an intermediate 1 M Ω resistance standard (open triangles). The standard uncertainty for each point is approximately 1 Ω .

standard. Calculations for these ratios yield combined standard uncertainties of approximately 0.07 $\mu\Omega/\Omega$ for 1 M Ω and 0.07 $\mu\Omega/\Omega$ for 10 M Ω with the same timing parameters as in Fig. 4 and Fig. 5.

IV. COMPARISON WITH EXPERIMENT

Type A uncertainties obtained with the bridge for a variety of bridge parameters are between one and two times the estimated combined standard uncertainty for the SQUID and Johnson noise contributions. This range of values reflects typical laboratory conditions and is reasonable given external noise sources.

Measurement results for a 10 M Ω resistor based on a direct scaling using the QHR standard agree with the 10-to-1 scaling between 10 M Ω and a calibrated 1 M Ω resistor within the estimated standard uncertainty. Figure 6 shows resistance values obtained for a 10 M Ω standard in direct ratio comparisons with the QHR standard at three voltage levels, and similar results based on a QHR-calibrated 1 M Ω standard. In this low voltage range the uncertainty in 10-to-1 scaling is dominated by 1/f noise in the DC SQUID detector. Results based on comparisons between 1 M Ω and 10 M Ω standards at a bridge voltage of 10 V agree with QHR-based comparison results to within the standard uncertainty of 0.05 $\mu\Omega/\Omega$.

Another test of the bridge type B uncertainty is to compare two scaling paths between resistors having a resistance ratio of 100-to-1. Direct ratios, using 100 M Ω and 1 M Ω standards, were compared to combined ratios based on two 10-to-1 ratios using an intermediate 10 M Ω standard. No significant differences were seen between these scaling paths to 100 M Ω , with a typical type A uncertainty of 0.15 $\mu\Omega/\Omega$ for a source voltage of 10 V. Similar results were obtained based on the 3100-to-310 winding ratio and the 310-to-31 ratio for the comparison of 1 M Ω and 10 M Ω standards, which agree at the level of

0.03 $\mu\Omega/\Omega \pm 0.05 \mu\Omega/\Omega$.

V. CONCLUSIONS

At present, the dominant uncertainty component in most of the measurement range is the 1/f noise component. The uncertainty calculation is in good agreement with the most sensitive results of 100-to-1 and 10-to-1 scaling measurements, and the uncertainty estimate shows that this CCC can achieve a combined standard uncertainty of order 0.1 $\mu\Omega/\Omega$ for resistors of 100 M Ω and 1 $\mu\Omega/\Omega$ for resistors of 1 G Ω with 10 V bridge voltage. Comparing this new CCC with traditional methods its combined standard uncertainty is two or three times smaller. But the great advantage of the two-terminal CCC is its scaling power. While with a traditional method the total uncertainty in a scaling process to high value resistor is the quadratic sum of the uncertainty in each step. The two-terminal CCC can measure a 10 M Ω resistor directly with the QHR, and its uncertainty at 10 M Ω is approximately 10 times lower than the best uncertainties claimed in the CCEM-K2 key comparison [14]. In further scaling, it is possible with this new method in only one step to scale to a resistor between 100 k Ω and 1 G Ω .

ACKNOWLEDGMENT

The authors are indebted to several collaborators who have made significant contributions to the development of the high-resistance CCC, including B. Pritchard of the National Measurement Institute (Australia), F. Hernandez-Marquez of the Centro Nacional de Metrología (Mexico), and G. R. Jones, Jr. of the National Institute of Standards and Technology.

REFERENCES

- [1] E. Pesel, B. Schumacher and P. Warnecke, "Resistance scaling up to 1 M Ω at PTB with a cryogenic current comparator," *IEEE Trans. Instrum. Meas.*, vol. 44, no. 2, pp. 273-275, Apr. 1995.
- [2] N. Feltn, L. Devoille, F. Piquemal, S. V. Lotkhov, and A. B. Zorin, "Progress in measurements of a single-electron pump by means of a CCC," *IEEE Trans. Instrum. Meas.*, vol. 52, no. 2, pp. 599-603, Apr. 2003.
- [3] R. E. Elmquist, "Leakage current detection in cryogenic current comparator bridges," *IEEE Trans. Instrum. Meas.*, vol. 42, no. 2, pp. 167-169, Apr. 1993.
- [4] R. E. Elmquist, E. Hourdakakis, D. G. Jarrett and N. M. Zimmerman, "Direct resistance comparisons from the QHR to 100 M Ω using a cryogenic current comparator," *IEEE Trans. Instrum. Meas.*, vol. 54, no. 2, pp. 525-528, Apr. 2005.
- [5] G. Rietveld, E. Bartolomé, J. Sesé, P. de la Court, J. Flokstra, C. Rillo, and A. Camón, "1:30 000 cryogenic current comparator with optimum SQUID readout," *IEEE Trans. Instrum. Meas.*, vol. 52, pp. 621-625, 2003.
- [6] R. E. Elmquist, G. R. Jones, Jr. B. Pritchard, M. E. Bierzychudek and F. Hernandez, "High resistance scaling from 10 k Ω and QHR standards using a cryogenic current comparator," CPEM 2008 Digest, p. 268-269, Broomfield, Colorado, USA, June 2008.
- [7] M. E. Bierzychudek, R. E. Elmquist, "Uncertainty Evaluation in a Two-Terminal Cryogenic Current Comparator," CPEM 2008 Digest, p. 152-153, Broomfield, Colorado, USA, June 2008.

- [8] B. V. Hamon, "A 1-100 Ω build-up resistor for the calibration of standard resistors," *J. Sci. Instrum.*, vol 31, pp. 450-453, 1954.
- [9] D. G. Jarrett, "Evaluation of guarded high resistance hamon transfer standards," *IEEE Trans. Instrum. Meas.*, vol. 48, pp. 324-328, Apr. 1999.
- [10] R. F. Dziuba, D. G. Jarrett, L. L. Scott, and A. J. Secula, "Fabrication of high-value standard resistors," *IEEE Trans. Instrum. Meas.*, vol. 48, pp. 333-337, Apr. 1999.
- [11] M. E. Bierzychudek, R. Garcia, M. Real and A. Tonina, "Design and fabrication of high value standard resistors at INTI," CPEM 2008 Digest, p. 396-397, Broomfield, Colorado, USA, June 2008.
- [12] F. Delahaye, "Series and parallel connection of multiterminal quantum Hall effect devices," *J. Appl. Phys.*, vol 73, pp. 7915-7920, 1993.
- [13] M. E. Cage, A. Jeffery, R. E. Elmquist and K. C. Lee, "Calculating the effect of longitudinal resistance in multi-series-connected quantum Hall effect devices," *J. Res. Natl. Inst. Stand. Technol.* 103, 561 (1998).
- [14] R. F. Dziuba and D. G. Jarrett, "CCEM-K2 Key Comparison of Resistance Standards at 10 M Ω and 1 G Ω ," July, 2001. Available

online at http://kcdb.bipm.org/AppendixB/appbresults/ccem-k2/ccem-k2_final_report.pdf

M. E. Bierzychudek received the electronics engineer degree from the Universidad de Buenos Aires, Argentina, in 2006.

In 2005, he joined the Electricity Division, Instituto Nacional de Tecnología Industrial, Argentina, and he has worked since then in the voltage and resistance laboratory; involved in measurements of the Josephson effect and the Quantum Hall effect.

R. E. Elmquist (M '90, SM '98) received the B. A. and Ph.D. degrees from the University of Virginia in Charlottesville, in 1979 and 1986, respectively.

In 1986, he joined the National Institute of Standards and Technology, in Gaithersburg, MD. His interests include development of cryogenic current comparator systems for resistance scaling, ac/dc calculable resistors, and SI measurements. He presently is the leader of the Metrology of the Ohm project in the Quantum Electrical Metrology Division of the Electronics and Electrical Engineering Laboratory.